Proceedings of 14th Symposium on Integrated Observing and Assimilation Systems for the Atmosphere, Oceans, and Land Surface (IOAS-AOLS), **Atlanta, 17-21 January 2010**

5B.1 A Fully Conserved Adjustment Scheme for Stabilization of Hydrographic Profiles

Peter C. Chu and Chenwu Fan
Department of Oceanography
Naval Postgraduate School
Monterey, CA 93943

Abstract

Hydrographic data, be it observational or averaged data, contain substantial regions having vertical density inversions. A new analytical conserved adjustment scheme has been developed on the base of conservation of heat, salt, and static stability for the whole water column with a predetermined (*T*, *S*) adjustment ratio. A set of well-posed combined linear and nonlinear algebraic equations has been established and is solved using the Newton's method. This new scheme can be used for ocean hydrographic data analysis and data assimilation.

1. Introduction

Raw and averaged observational hydrographic data contain substantial regions having vertical density inversions. For example, Jackett and McDougall (1995) found that the annually averaged field of the Ocean Atlas of Levitus (1982) had more than 44% of the casts possessing static instability at least at one level. Here, the word 'cast' is used to denote a pair of vertical temperature and salinity profiles. A widely used concept for static stability (E) is defined by Lynn and Reid (1968) as "the individual density gradient by vertical displacement of a water parcel (as opposed to the geometric density gradient)." For discrete samples (T_k, S_k) at depth z_k, k = 1, 2, …, K (k increasing downward), the density difference between two adjacent levels is taken after one is adiabatically displaced to the depth of the other. Computationally, E_k is calculated by

$$E_k = \rho(S_{k+1}, T_{k+1}, z_k) - \rho(S_k, T_k, z_k), \quad k = 1, 2, \ldots, K\text{-}1 \quad (1)$$

where $\rho(S_{k+1}, T_{k+1}, z_k)$ is the local potential density of the lower of the two adjacent levels between z_k and z_{k+1} with respect to the upper of the two adjacent levels (z_k); and ρ is the in-situ density to the depth of the upper of the two adjacent levels (z_k). The density inversion is defined by the occurrence of negative value of E_k. The minimum static stability is represented by $E_k = 0$. It is not always possible to reach zero exactly due to the precision limitations of the temperature and salinity values used. As a result, the minimum value for the static stability is given by

$$E_k \geq E_{\min}, \quad k = 1, 2, ..., K, \quad (2)$$

where $E_{\min}$ is the reference value for the minimum static stability. If static instability occurs in an observed or averaged hydrographic cast [i.e., (2) does not satisfy], this profile need to be adjusted.

The National Ocean Data Center (NODC) uses a local interactive (*T*, *S*) separated adjustment method, which is based on the method proposed by Jackett and McDougall (1995) (hereafter referred to JM method) to minimally alter climatological temperature and salinity profiles to achieve a stable water column everywhere in the world ocean. Before deciding which level to change, the values of $\partial T/\partial z$ and $\partial S/\partial z$, the gradient of temperature and salinity between two adjacent levels involve in the instability, are examined. This helps determine if the temperature or salinity profile, or both, are to be changed to stabilize the density field. If $\partial T/\partial z < 0$, $\partial S/\partial z < 0$, only temperature is changed; If $\partial T/\partial z > 0$, $\partial S/\partial z > 0$, only salinity is changed; If $\partial T/\partial z < 0$, $\partial S/\partial z > 0$, both temperature and salinity fields are adjusted with a local linear trend test (Locarnini et al. 2006). Here, z-axis points upward. The principal is to stabilize the hydrographic profiles with minimum adjustment.

The benefit of using the JM method can be easily identified from comparison between two ocean atlases: Ocean Atlas of Levitus (1982) (without the JM adjustment) and World Ocean Atlas 2005 (Locarnini et al. 2006) (with the JM adjustment). Both atlases consist of annually and monthly averaged vertical profiles of temperature and salinity on a global $1^o \times 1^o$ grid at 33 vertical levels. The Ocean Atlas of Levitus (1982) has considerable casts possessing static instability. However, the World Ocean Atlas 2005 contains no profile possessing static instability.

Although eliminating the static instability, the JM method does not require the conservation of heat and salt. Since one of ocean's important roles in the earth's climate is heat transport, the adjustment without taking into account of heat conservation may lead to error in estimating the ocean's impact on global climate change. In this study, a new conserved scheme is developed to simultaneously adjust the temperature and salinity profiles from (T_k, S_k) to ($T_k + \Delta T_k, S_k + \Delta S_k$). A set of 2$K$ algebraic (linear and nonlinear) equations are established to get ($\Delta T_k, \Delta S_k$) on the base of heat and salt conservation, predetermined ($\Delta T_k / \Delta S_k$) ratios (or called adjustment ratios) for all levels, and removal of static instability by adjusting Ek to $E_k + \Delta E_k$ with a combined conservation and non-uniform increment treatment.

2. Unconserved Adjustment

An example as described in Appendix B of Locarnini et al. (2006) is used for illustration. The area chosen for this example is the one-degree latitude-longitude box centered at 53.5°S -171.5°E from a previous version of the World Ocean Atlas 1998 (WOA98). This is on the New Zealand Plateau, with a bottom depth below 1000 m and above 1100 m. The month is October, during the early austral summer. There is no temperature or salinity data within the chosen one-degree box. Thus the objectively analyzed values in this one-degree box will be dependent on the seasonal objectively analyzed field and the data in nearby one-degree grid boxes. There is much more temperature data than salinity data on the New Zealand plateau for October. This contributes to six small (on the order of 10^{-2} kg m^{-3}) inversions in the local potential density field calculated from objectively analyzed temperature and salinity fields (Table 1). After using the JM method, the original and adjusted profiles {T_k, S_k, k =1, 2, …, K} are as shown in Fig. 1, and the adjusted temperature and salinity profiles are listed in Table 2. Readers are referred to Appendix B of Locarnini et al. (2006) for detailed information on the stabilization procedures. The relative root mean adjustment (RRMA) can be represented by

$$\text{RRMA} = \frac{\sqrt{\frac{1}{K}\sum_{k=1}^{K}(\Delta T_k)^2}}{\max(T_k) - \min(T_k)} + \frac{\sqrt{\frac{1}{K}\sum_{k=1}^{K}(\Delta S_k)^2}}{\max(S_k) - \min(S_k)}$$

$$= 0.0712. \qquad (3)$$

The total heat and salt changes of the water column within this $1^o \times 1^o$ grid box are estimated by

$$\Delta Q = A\rho_0 c_p \int_{-H}^{0} \Delta T dz, \quad \Delta(\text{Salt}) = A \int_{-H}^{0} \Delta S dz,$$

where ρ_0 (=1028 kg m-3) is the characteristic density, c_p (= 4002 J kg^{-1} K^{-1}) is the specific heat for the sea water, H = 1000 m, and A is the area of the grid box,

$$A = (\frac{\pi}{180} R)^2 \cos\varphi,$$

where R (= 6370 km) is the earth radius, and φ (=53.5°) is the latitude of the grid box. The temperature and salinity adjustments ($\Delta T, \Delta S$) are obtained by comparison between Table 1 and Table 2, the heat and salt changes of the water column for this grid box are calculated by

$$\Delta Q = -7.0411 \times 10^{17} \text{ J}, \quad \Delta(\text{salt}) = -0.5443 \times 10^{10} \text{ kg}.$$

Since one of the ocean's important roles in the earth's climate is transporting heat from low to high latitudes, nontrivial heat and salt losses show that the unconserved adjustment may change heat transport and in turn affect the overturning thermohaline circulation.

3. Stabilization

The stabilization process is divided into three parts: (a) stability increasing at unstable levels, (b) stability decreasing at stable levels, (c) normalization for conservation of stability for the cast. Let static instability occur at level k_1, k_2, …, k_i [i.e., satisfies the inequality (2)], the static stability E_{k_i} is increased to its marginal stability value ($E^*_{k_i}$),

$$E^*_{k_i} = E_{\min}, \qquad (4)$$

with increments of $\Delta E_{k_i} = E_{\min} - E_{k_i}$.

Such an increase of stability will be compensated by the decrease of stability at neighboring levels $k_i \pm m$ (m = 1, 2, …) with skipping the unstable levels until reaching the top and bottom of the profile,

$$E^*_{k_i \pm m} = \begin{cases} E_{k_i \pm m} - \Delta E_{k_i} / 2^{m+1} & \text{if } E_{k_i \pm m} - \Delta E_{k_i} / 2^{m+1} \geq E_{\min} \\ E_{\min} & \text{if } E_{k_i \pm m} - \Delta E_{k_i} / 2^{m+1} < E_{\min} \end{cases} \quad (5)$$

The static stabilities for the whole profile before and after the adjustment is calculated by

$$I = \sum_{k=1}^{K} E_k, \; I^* = \sum_{k=1}^{K} E_k^* . \quad (6)$$

The normalization process is conducted by

$$E_k^{**} = \frac{I}{I^*} E_k^* . \quad (7)$$

After these three processes conducted for stabilization, the static stability is represented by [see Eq.(1)]

$$\rho(S_{k+1} + \Delta S_{k+1}, T_{k+1} + \Delta T_{k+1}, z_k) - \rho(S_k + \Delta S_k, T_k + \Delta T_k, z_k) = E_k^{**}, \; k = 1, 2, ..., K\text{-}1. \quad (8)$$

4. Constraints for Temperature and Salinity Adjustment

Two types of constraints are used: conservation and predetermined adjustment ratios. Conservation of heat and salt for the adjustment can be represented by

$$\int_{-h}^{0} \Delta T dz = 0, \quad \int_{-h}^{0} \Delta S dz = 0, \quad (9)$$

which can be discretized by

$$\sum_{k=1}^{K-1} \frac{(\Delta T_k + \Delta T_{k+1})}{2} (z_k - z_{k+1}) = 0 , \quad (10)$$

$$\sum_{k=1}^{K-1} \frac{(\Delta S_k + \Delta S_{k+1})}{2} (z_k - z_{k+1}) = 0 . \quad (11)$$

The adjustment ratios ($\Delta T_k / \Delta S_k = -\gamma_k$, the negative sign is used due to opposite effects of T, S on the density, $\gamma_k > 0$) are predetermined empirically for N-1 levels.

$$\Delta T_k + \gamma_k \Delta S_k = 0 , \quad k = 1, 2, \ldots, K\text{-}1. \quad (12)$$

Eqs.(10), (11), (12), and (8) represent a set of 2K algebraic equations for ($\Delta T_k, \Delta S_k$), k = 1, 2, …, K. Among them, (8) is nonlinear and (10), (11), (12) are linear. The Newton method is used to solve the set of 2K algebraic equations.

5. Newton Method

Let the temperature and salinity adjustment be represented by a 2K-dimensional vector P,

$$\mathbf{P} \equiv \begin{bmatrix} p_1 \\ p_2 \\ p_3 \\ p_4 \\ \vdots \\ \vdots \\ \vdots \\ p_{M-1} \\ p_M \end{bmatrix} = \begin{bmatrix} \Delta T_1 \\ \Delta S_1 \\ \Delta T_2 \\ \Delta S_2 \\ \vdots \\ \vdots \\ \vdots \\ \Delta T_K \\ \Delta S_K \end{bmatrix}, \qquad M = 2K. \quad (13)$$

The algebraic equations (10), (11), (12), (8) [note that we put (8) at the last] can be represented by

$$\mathbf{F}(\mathbf{P}) = 0 , \quad (14)$$

where **F** has the dimension of 2*K*. The classical Newton Method for approximating a desired solution P to (14) is formally defined by the iteration

$$\mathbf{P}^{(j+1)} = \mathbf{P}^{(j)} - \mathbf{J}_F^{-1}(\mathbf{P}^{(j)}) \mathbf{F}(\mathbf{P}^{(j)}), \; j = 0, 1, 2, ... \quad (15)$$

where $\mathbf{P}^{(j)}$ is the j-th approximation to the solution of (14), $\mathbf{J}_F(\mathbf{P}^{(j)})$ is the Jacobian matrix of $\mathbf{F}(\mathbf{P})$ evaluated at $\mathbf{P}^{(j)}$. Inversion of the Jacobian matrix is not performed in practice: rather (15) is implemented via solution of the following system of linear equations at each iteration,

$$\mathbf{J}_F(\mathbf{P}^{(j)}) \bullet \mathbf{d}^{(j)} = \mathbf{b}^{(j)}, \quad \mathbf{b}^{(j)} \equiv -\mathbf{F}(\mathbf{P}^{(j)}), \quad (16)$$

followed by the update

$$\mathbf{P}^{(j+1)} = \mathbf{P}^{(j)} + \mathbf{d}^{(j)} , \quad (17)$$

where $\mathbf{d}^{(j)}$ is called the Newton direction. The iteration stops at step J when

$$\max_k \left| d_k^{(J)} \right| < 10^{-6} \quad (^{\circ}\text{K for temperature and ppt for salinity}) . \quad (18)$$

When the set of algebraic equations take the order of (10), (11), (12), and (8), the Jacobian matrix $\mathbf{J}_F(\mathbf{P}^{(j)})$ with dimension of $M \times M$ is represented by

$$\mathbf{J}_F(\mathbf{P}^{(j)}) = \begin{bmatrix} a_{11} & a_{12} & ... & a_{1M} \\ a_{21} & a_{22} & ... & a_{2M} \\ ... & ... & ... & ... \\ a_{M1} & a_{M2} & ... & a_{MM} \end{bmatrix}, \qquad (19)$$

where the M × M elements are given in (A1) of Appendix A. The Jacobian matrix (18) has the following format with many zero elements,

$$\mathbf{J}_F(\mathbf{P}^{(j)}) = \begin{bmatrix} * & 0 & * & 0 & * & 0 & ... & ... & * & 0 \\ 0 & * & 0 & * & 0 & * & ... & ... & 0 & * \\ * & * & 0 & 0 & 0 & 0 & ... & ... & 0 & 0 \\ * & * & * & * & 0 & 0 & ... & ... & 0 & 0 \\ 0 & 0 & * & * & 0 & 0 & ... & ... & 0 & 0 \\ 0 & 0 & * & * & * & * & ... & ... & 0 & 0 \\ ... & ... & ... & ... & ... & ... & ... & ... & ... & ... \\ ... & ... & ... & ... & ... & ... & ... & ... & ... & ... \\ 0 & 0 & 0 & 0 & ... & ... & * & * & 0 & 0 \\ 0 & 0 & 0 & 0 & ... & ... & * & * & * & * \end{bmatrix}, \qquad (20)$$

where nonzero elements are indicated by the symbol '*'. The vector b in the righthand-side of (16) has the following components:

$$\begin{aligned} & b_1 = 0, \quad b_2 = 0, \quad b_3 = 0, \\ & b_4 = E_1^{**} - \rho\left(S_1 + \Delta S_1^{(j)}, T_1 + \Delta T_1^{(j)}, z_1\right) \\ & + \rho\left(S_2 + \Delta S_2^{(j)}, T_2 + \Delta T_2^{(j)}, z_2\right), \\ & b_5 = 0, \\ & b_6 = E_2^{**} - \rho\left(S_2 + \Delta S_2^{(j)}, T_2 + \Delta T_2^{(j)}, z_2\right) \\ & + \rho\left(S_3 + \Delta S_3^{(j)}, T_3 + \Delta T_3^{(j)}, z_2\right), ..., \\ & b_{M-1} = 0, \\ & b_M = E_{K-1}^{**} - \rho\left(S_{K-1} + \Delta S_{K-1}^{(j)}, T_K + \Delta T_{K-1}^{(j)}, z_{K-1}\right) \\ & + \rho\left(S_K + \Delta S_K^{(j)}, T_K + \Delta T_K^{(j)}, z_{K-1}\right). \end{aligned} \qquad (21)$$

It is noted that the well-posed linear algebraic equation (16) is easily solved with the initial guess,

$$\mathbf{P}^{(0)} = 0, \qquad (22)$$

i.e.,

$$\Delta T_k^{(0)} = 0, \quad \Delta S_k^{(0)} = 0, \quad k = 1, 2, ..., K. \qquad (23)$$

The free parameters for this adjustment method are the reference value for the minimum static stability ($E_{\min}$) and the T-S adjustment ratios $\{\gamma_k, k = 1, 2, \ldots, N\}$. The same value is used as in Locarnini et al. (2006) for $E_{\min}$ in this study,

$$E_{\min} = 10^{-4}\ \text{kg m}^{-3}. \qquad (24)$$

After several tests, we found that use of the following depth independent ratio

$$\gamma_k = \gamma \equiv \frac{\max(T_k) - \min(T_k)}{\max(S_k) - \min(S_k)}, \qquad (25)$$

the Newton process (17) converges in few steps.

6. Example

The same example as described in Section 2 is used for illustration. Substitution of $\{S_k, T_k, z_k\}$ values from Table 1 into (20) and (21) with the initial guess (23), the Newton direction $\mathbf{d}^{(0)}$ is obtained from solving the linear algebraic equation (16). The vector $\mathbf{d}^{(0)}$ is added to the initial guess $\mathbf{P}^{(0)}$, which leads to

$$\mathbf{P}^{(1)} = \mathbf{P}^{(0)} + \mathbf{d}^{(0)} \qquad (26)$$

With $\mathbf{P}^{(1)}$, the cast is adjusted to its first iterated values,

$$S_k^{(1)} = S_k + \Delta S_k^{(1)}, \quad T_k^{(1)} = T_k + \Delta T_k^{(1)}. \qquad (27)$$

Substitution of (26) into (1) gives static stability after first iteration $E_k^{(1)}$. If

$$E_k^{(1)} \geq E_{\min}, \quad k = 1, 2, ..., K, \qquad (28)$$

the adjustment stops. Otherwise, the iteration continues, i.e., the linear algebraic equation (16) is solved after using $\mathbf{P}^{(1)}$ from (26). Addition of the solution $\mathbf{d}^{(1)}$ to $\mathbf{P}^{(1)}$ leads to $\mathbf{P}^{(2)}$. If there is no static instability, the adjustment stops. Otherwise, the iteration continues until the static instability is eliminated. For the hydrographic cast listed in Table1, only three iterations are needed to eliminate the static instability. Tables 3 and 4 list the values of $\{T_k, S_k\}$ at the each iteration. They show the high efficiency of this method for elimination of static instability in hydrographic cast. Fig. 2 shows the original and adjusted profiles {Sk, T_k, E_k}, k =1, 2, …, K. The heat and salt are conserved for the whole water column with the relative root-mean adjustment

$$\text{RRMA} = 0.0482. \qquad (29)$$

Comparing (29) to (3), we may find that this analytical conserved adjustment scheme has a smaller RRMA (0.0482) than the JM method (0.0712).

7. Application to Data Assimilation in Ocean Modeling

Data assimilation is required in operational ocean data access and retrieval (Sun 1999). It is to blend the

modeled variable ($\mathbf{x}_m$) with observational data ($\mathbf{y}_o$) (e.g., Lozano et al. 1996, Chu et al. 2004),

$$\mathbf{x}_a = \mathbf{x}_m + \mathbf{W} \bullet \left[\mathbf{y}_o - H(\mathbf{x}_m)\right], \qquad (30)$$

where $\mathbf{x}_a$ is the assimilated variable; H is an operator that provides the model's theoretical estimate of what is observed at the observational points, and W is the weight matrix. Difference among various data assimilation schemes such as optimal interpolation (e.g., Barron and Kara 2006), Kalman filter (e.g., Galanis et al. 2006), and variation methods (e.g., Tang and Kleeman 2004) is the different ways to determine the weight matrix W. The data assimilation process (30) can be considered as the average (in a generalized sense) of $\mathbf{x}_m$ and $\mathbf{y}_o$. In ocean (T, S) data assimilation, the observational data ($\mathbf{y}_o$) may contain several casts, which are statically stable. The model profile ($\mathbf{x}_m$) is also statically stable since convective adjustment (Bryan 1969) is usually conducted at each time step.

False static stability may be generated after (T, S) data assimilation [i.e., performing (30)]. For example, 10-day JPL Estimating the Circulation and Climate of the Ocean (ECCO) (T, S) fields centered on 31 December 2008 (download from the website: http://ecco.jpl.nasa.gov/external/) show considerable portion (11.57%) of profiles are statically unstable (Fig. 3). Here, the National Ocean Data Center's criterion for flagging out statically unstable profiles,

$$E(k) < \begin{cases} -0.03 \ \text{kg m}^{-3} & (0 \geq z_k \geq -30 \ \text{m}) \\ -0.02 \ \text{kg m}^{-3} & (-30 \ \text{m} > z_k \geq -400m) \\ 0 \ \text{kg m}^{-3} & (-400 \ \text{m} > z_k) \end{cases}, \qquad (31)$$

is used. Since such a false static instability is due to the blending of observational data with the model data, not a real instability. Use of the convective adjustment scheme may over-correct the profiles.

To illustrate this, we discuss the existing convective adjustment schemes in ocean models. The various convective adjustment schemes are based on the same original idea (e.g., Bryan 1969): whenever a water column is statically unstable, temperature and salinity are vertically adjusted to make the water column neutrally stable, with heat and salt conserved in the process. The adjustment takes an iterative approach. The iteration continues between all adjacent levels until the static instability is removed in the whole water column. Because the adjustment acts on only neighboring points, the number of iterations required to reach the final stable state is infinite for a given unstable profile (Smith 1989). In practice, however, the number of iteration is always finite, and this leads to some residual instabilities (Killworth 1989).

Several algorithms were developed to remove these residual static instabilities such as the implicit vertical diffusion scheme (Cox 1984; Killworth 1989) and the complete adjustment scheme (Yin and Sarachik 1994). The former tests the static stability between the vertically adjacent levels and, if unstable, the vertical diffusivity is set to a large value (convective diffusivity) in order to smooth out the instability. The latter is to determine the upper and lower boundaries of each adjusted region while keeping the instantaneous adjustment within each unstable region. Yin and Sarachik (1994) showed that the complete convective adjustment scheme is more efficient than the implicit vertical diffusion scheme and guarantees a complete removal of static instability of a water column at each time step. For the same example as described in Section 2, the complete convective adjustment scheme removes the static instabilities (Fig. 4) with the relative root-mean adjustment,

$$\text{RRMA} = 0.2192. \qquad (32)$$

This value is 4.5 times larger than that (0.0482) using the analytical adjustment method.

8. Conclusions

A new analytical conserved adjustment scheme is developed to eliminate static instability of raw and averaged observational hydrographic data. This method adjusts the temperature and salinity profiles $\{\Delta T_k, \Delta S_k, \ k = 1, 2, ..., K\}$ simultaneously and efficiently on the base of three types of constraints: (a) heat and salt conservation, (b) predetermined ($\Delta T_k / \Delta S_k$) ratios (or called adjustment ratios) for all levels, and (c) removal of static instability by adjusting the static stability with a combined conservation and non-uniform increment treatment. With these constraints, a set of $2K$ combined linear/nonlinear algebraic equations are established for $\{\Delta T_k, \Delta S_k\}$. Among them, ($K$ + 1) algebraic equations are linear, (K – 1) equations are nonlinear. The Newton's method is used to solve this set of equations with few steps of iteration. This scheme has very small relative root-mean square adjustment compared to the existing methods.

This scheme has three features: (1) conservation of heat and salt, (2) removal of static instabilities with small (T, S) adjustments, and (3) analytical form. With these features, it is can be widely used in ocean (T, S) data analysis. Besides, ocean data assimilation may cause false static instabilities. Since this instability is not real, minimal adjustment to stabilize the cast is ideal. The analytical

conserved adjustment scheme can be used in ocean (T, S) data assimilation.

Acknowledgments

The Office of Naval Research, the Naval Oceanographic Office, and the Naval Postgraduate School supported this study.

Appendix A Elements of Jacobian Matrix (19)

The elements of M × M Jacobian matrix (19) are given by

$$a_{11} = \frac{\Delta z_1}{2}, a_{13} = \frac{\Delta z_1 + \Delta z_2}{2}, ..., a_{1,M-3} = \frac{\Delta z_{N-2} + \Delta z_{N-1}}{2},$$

$$a_{1,M-1} = \frac{\Delta z_{N-1}}{2}, a_{12} = a_{14} = a_{16} = ... = a_{1M} = 0,$$

$$a_{22} = \frac{\Delta z_1}{2}, a_{24} = \frac{\Delta z_1 + \Delta z_2}{2}, ..., a_{2,M-2} = \frac{\Delta z_{N-2} + \Delta z_{N-1}}{2},$$

$$a_{2M} = \frac{\Delta z_{N-1}}{2}, a_{21} = a_{23} = a_{25} = ... = a_{2,M-1} = 0,$$

$$a_{31} = 1,\ a_{32} = \gamma_1,\ \ a_{33} = a_{34} = a_{35} = ... = a_{3M} = 0$$

$$a_{41} = \frac{\partial \rho\left(S_1 + \Delta S_1^{(j)}, T_1 + T_1^{(j)}, z_2\right)}{\partial T}$$
$$= -\rho\left(S_1 + \Delta S_1^{(j)}, T_1 + \Delta T_1^{(j)}, z_2\right)\alpha\left(S_1 + \Delta S_1^{(j)}, T_1 + \Delta T_1^{(j)}, z_2\right),$$

$$a_{42} = \frac{\partial \rho\left(S_1 + \Delta S_1^{(j)}, T_1 + \Delta T_1^{(j)}, z_2\right)}{\partial S}$$
$$= \rho\left(S_1 + \Delta S_1^{(j)}, T_1 + \Delta T_1^{(j)}, z_2\right)\beta\left(S_1 + \Delta S_1^{(j)}, T_1 + \Delta T_1^{(j)}, z_2\right),$$

$$a_{43} = -\frac{\partial \rho\left(S_2 + \Delta S_2^{(j)}, T_2 + \Delta T_2^{(j)}, z_2\right)}{\partial T}$$
$$= \rho\left(S_2 + \Delta S_2^{(j)}, T_2 + \Delta T_2^{(j)}, z_2\right)\alpha\left(S_2 + \Delta S_2^{(j)}, T_2 + \Delta T_2^{(j)}, z_2\right),$$

$$a_{44} = -\frac{\partial \rho\left(S_2 + \Delta S_2^{(j)}, T_2 + \Delta T_2^{(j)}, z_2\right)}{\partial S}$$
$$= -\rho\left(S_2 + \Delta S_2^{(j)}, T_2 + \Delta T_2^{(j)}, z_2\right)\beta\left(S_2 + \Delta S_2^{(j)}, T_2 + \Delta T_2^{(j)}, z_2\right),$$

$$a_{45} = a_{46} = ... = a_{4M} = 0,$$

$$a_{53} = 1,\ \ a_{54} = \gamma_2,$$

$$a_{51} = a_{52} = a_{55} = a_{56} = a_{57} = ... = a_{5M} = 0,$$

$$a_{63} = \frac{\partial \rho\left(S_2 + \Delta S_2^{(j)}, T_2 + \Delta T_2^{(j)}, z_3\right)}{\partial T}$$
$$= -\rho\left(S_2 + \Delta S_2^{(j)}, T_2 + \Delta T_2^{(j)}, z_3\right)\alpha\left(S_2 + \Delta S_2^{(j)}, T_2 + \Delta T_2^{(j)}, z_3\right),$$

$$a_{64} = \frac{\partial \rho\left(S_2 + \Delta S_2^{(j)}, T_2 + \Delta T_2^{(j)}, z_3\right)}{\partial S}$$
$$= \rho\left(S_2 + \Delta S_2^{(j)}, T_2 + \Delta T_2^{(j)}, z_3\right)\beta\left(S_2 + \Delta S_2^{(j)}, T_2 + \Delta T_2^{(j)}, z_3\right),$$

$$a_{65} = -\frac{\partial \rho\left(S_3 + \Delta S_3^{(j)}, T_3 + \Delta T_3^{(j)}, z_3\right)}{\partial T}$$
$$= \rho\left(S_3 + \Delta S_3^{(j)}, T_3 + \Delta T_3^{(j)}, z_3\right)\alpha\left(S_3 + \Delta S_3^{(j)}, T_3 + \Delta T_3^{(j)}, z_3\right),$$

$$a_{66} = -\frac{\partial \rho\left(S_3 + \Delta S_3^{(j)}, T_3 + \Delta T_3^{(j)}, z_3\right)}{\partial S}$$
$$= -\rho\left(S_3 + \Delta S_3^{(j)}, T_3 + \Delta T_3^{(j)}, z_3\right)\beta\left(S_3 + \Delta S_3^{(j)}, T_3 + \Delta T_3^{(j)}, z_3\right),$$

$$a_{61} = a_{62} = a_{67} = a_{68} = ... = a_{6M} = 0,$$

.....

$$a_{M-1,M-3} = 1,\ \ a_{M-1,M-2} = \gamma_{N-1},$$

$$a_{M-1,1} = a_{M-1,2} = ... = a_{M-1,M-4} = a_{M-1,M-1} = a_{M-1,M} = 0,$$

$$a_{M,M-3} = \frac{\partial \rho\left(S_{K-1} + \Delta S_{K-1}^{(j)}, T_{K-1} + \Delta T_{K-1}^{(j)}, z_K\right)}{\partial T}$$
$$= -\rho\left(S_{K-1} + \Delta S_{K-1}^{(j)}, T_{K-1} + \Delta T_{K-1}^{(j)}, z_K\right)$$
$$\times\alpha\left(S_{K-1} + \Delta S_{K-1}^{(j)}, T_{K-1} + \Delta T_{K-1}^{(j)}, z_K\right),$$

$$a_{M,M-2} = \frac{\partial \rho\left(S_{K-1} + \Delta S_{K-1}^{(j)}, T_{K-1} + \Delta T_{K-1}^{(j)}, z_K\right)}{\partial S}$$
$$= \rho\left(S_{K-1} + \Delta S_{K-1}^{(j)}, T_{K-1} + \Delta T_{K-1}^{(j)}, z_K\right)$$
$$\times\beta\left(S_{K-1} + \Delta S_{K-1}^{(j)}, T_{K-1} + \Delta T_{K-1}^{(j)}, z_K\right),$$

$$a_{M,M-1} = -\frac{\partial \rho\left(S_K + \Delta S_K^{(j)}, T_K + \Delta T_K^{(j)}, z_K\right)}{\partial T}$$
$$= \rho\left(S_K + \Delta S_K^{(j)}, T_K + \Delta T_K^{(j)}, z_K\right)$$
$$\times\alpha\left(S_K + \Delta S_K^{(j)}, T_K + \Delta T_K^{(j)}, z_K\right),$$

$$a_{MM} = -\frac{\partial \rho\left(S_K + \Delta S_K^{(j)}, T_K + \Delta T_K^{(j)}, z_K\right)}{\partial S}$$
$$= -\rho\left(S_K + \Delta S_K^{(j)}, T_K + \Delta T_K^{(j)}, z_K\right)$$
$$\times \beta\left(S_K + \Delta S_K^{(j)}, T_K + \Delta T_K^{(j)}, z_K\right),$$
$$a_{1M} = a_{2,M} = ... = a_{M-4,M} = 0. \qquad \text{(A1)}$$

References

Barron, C. N., and A. B. Kara, 2006: Satellite-based daily SSTs over the global ocean. Geophys. Res. Lett., 33, L15603, doi:10.1029/2006GL026356.

Bryan, K., 1969: A numerical method for the study of the circulation of the world ocean. J. Comput. Phys., 4, 347-376.

Chu, P.C., G.H. Wang, and C.W. Fan, 2004: Evaluation of the U.S. Navy's Modular Ocean Data Assimilation System (MODAS) using the South China Sea Monsoon Experiment (SCSMEX) data. J. Oceanogr., 60, 1007-1021.

Cox, M., 1984: A primitive equation, three-dimensional model of the ocean. GFDL Ocean Group Tech. Report No 1.

Galanis, G.N., P. Louka, P. Katsafados, G. Kallos and I. Pytharoulis, 2006: Applications of Kalman filters based on non-linear functions to numerical weather predictions. Ann. Geophys., 24, 2451-2460.

Jackett, D. R., and T. J. McDougall, 1995: Minimal adjustment of hydrographic profiles to achieve static stability. J. Atmos. Ocean. Technol., 12, 381-389.

Killworth, P.D., 1989: On the parameterization of deep convection in ocean models. Aha Huliko'a: Parameterization of Small Scale Processes, P. Muller, Ed., Hawaii Institute of Geophysics, 59-74.

Levitus, S., 1982: Climatological Atlas of the World Ocean. NOAA Professional Paper 13, 173 pp.

Locarnini, R. A., A. V. Mishonov, J. I. Antonov, T. P. Boyer, and H. E. Garcia, 2006: World Ocean Atlas 2005, Vol 1: Temperature. S. Levitus, Ed., NOAA Atlas NESDIS 61, 38 pp.

Lozano, C. J., A.R. Robinson, H.G. Arrango, A. Gangopadhyay, Q. Sloan, P. J. Haley, L. Anderson, and W. Leslie, 1996: An interdisplinary ocean prediction system: assimilation strategies and structured data models. Modern Approaches to Data Assimilation in Ocean Modeling, P. Malanotte-Rizzoli, Ed., Elsevier, Amsterdam, 413-452.

Lynn, R. G., and J. L. Reid, 1968: Characteristics and circulation of deep and abyssal waters. Deep-Sea Res., 15, 577-598.

Smith, N., 1989: The southern ocean thermohaline circulation: A numerical study. J. Phys. Oceanogr., 19, 713-726.

Sun, L.C., 1999: Data inter-operability driven by oceanic data assimilation needs. Mar. Technol. Soc. J., 33 (3), 55-66.

Tang, Y., and R. Kleeman, 2004: SST assimilation experiments in a tropical Pacific ocean model. J. Phys. Oceanogr., 34, 623-642.

Yin, F. L., and E. S. Sarachik, 1994: An efficient convective adjustment scheme for ocean circulation models. J. Phys. Oceanogr., 24, 1425 – 1430.

Table 1. Grid-box 171.5°E, 53.5°S WOA98 profiles before stabilization (from Locarnini et al. 2006, Table B1). Here the symbol '*' in the last column indicates the static instability.

k	Depth (m)	T (^{o}C)	S (ppt)	$\rho(S_{k+1}, T_{k+1}, z_k)$ (kg m^{-3})	$\rho(S_k, T_k, z_k)$ (kg m^{-3})	E_k (kg m^{-3})
1	0	7.1667	34.4243	26.9476	26.9423	0.0054
2	10	7.1489	34.4278	26.8982	26.9939	-0.0957*
3	20	7.0465	34.2880	26.9529	26.9443	0.0085
4	30	7.0050	34.2914	27.0104	26.9990	0.0114
5	50	6.9686	34.2991	27.0967	27.1028	-0.0061*
6	75	7.0604	34.3073	27.2406	27.2120	0.0286
7	100	6.9753	34.3280	27.3892	27.3560	0.0332
8	125	6.9218	34.3604	27.5164	27.5046	0.0117
9	150	6.8919	34.3697	27.6000	27.6316	-0.0316*
10	200	6.9363	34.3364	27.8123	27.8302	-0.0179*
11	250	7.0962	34.3415	28.0295	28.0421	-0.0126*
12	300	7.1622	34.3367	28.2684	28.2593	0.0092
13	400	6.8275	34.2852	28.6664	28.7281	-0.0618*
14	500	7.4001	34.3123	29.3699	29.1238	0.2461
15	600	6.2133	34.4022	29.9386	29.8292	0.1094
16	700	5.9186	34.4868	30.5869	30.3978	0.1891
17	800	4.5426	34.4904	31.0754	31.0488	0.0266
18	900	4.1263	34.4558	31.6539	31.5377	0.1162
19	1000	3.3112	34.4755		32.1176	

Table 2. Grid-box 171.5°E, 53.5°S WOA98 profiles after stabilization using the JM method (from Locarnini et al. 2006, Table B2).

k	Depth (m)	T (^{o}C)	S (ppt)	$\rho(S_{k+1}, T_{k+1}, z_k)$ (kg m^{-3})	$\rho(S_k, T_k, z_k)$ (kg m^{-3})	E_k (kg m^{-3})
1	0	7.1667	34.3096	26.8521	26.8519	0.0002
2	10	7.1489	34.3063	26.8982	26.8982	0.0000
3	20	7.0465	34.2880	26.9529	26.9443	0.0085
4	30	7.0050	34.2914	27.0042	26.9990	0.0051
5	50	7.0132	34.2991	27.0967	27.0967	0.0000
6	75	7.0604	34.3073	27.2361	27.2120	0.0240
7	100	6.9796	34.3228	27.3513	27.3513	0.0000
8	125	6.9897	34.3243	27.4667	27.4667	0.0000
9	150	7.0242	34.3301	27.5820	27.5820	0.0000
10	200	7.0628	34.3364	27.8123	27.8123	0.0000
11	250	7.0962	34.3415	28.0422	28.0421	0.0000
12	300	7.0748	34.3367	28.2719	28.2719	0.0001
13	400	6.8275	34.2894	28.7314	28.7314	0.0000
14	500	6.9604	34.3123	29.3699	29.1899	0.1799
15	600	6.2133	34.4022	29.9386	29.8292	0.1094
16	700	5.9186	34.4868	30.5869	30.3978	0.1891
17	800	4.5426	34.4904	31.0754	31.0488	0.0266
18	900	4.1263	34.4558	31.6539	31.5377	0.1162
19	1000	3.3112	34.4755		32.1176	

Table 3. Change of ($T_k + \Delta T_k^{(j)}$) (ºC) at each iteration using the Newton's method. It is noted that the iteration converges at the third iteration.

k	Depth (m)	j = 0	j = 1	j = 2	j = 3	j = 4
1	0	7.166700	7.212634	7.212833	7.212833	7.212833
2	10	7.148900	7.289401	7.289072	7.289072	7.289072
3	20	7.046500	6.818173	6.816828	6.816828	6.816828
4	30	7.005000	6.872865	6.872591	6.872591	6.872591
5	50	6.968600	6.888794	6.888861	6.888861	6.888861
6	75	7.060400	7.023494	7.023712	7.023712	7.023712
7	100	6.975300	6.977379	6.977638	6.977638	6.977638
8	125	6.921800	6.965175	6.965378	6.965378	6.965378
9	150	6.891900	6.983992	6.983997	6.983997	6.983997
10	200	6.936300	6.959537	6.959779	6.959779	6.959779
11	250	7.096200	7.125999	7.126229	7.126229	7.126229
12	300	7.162200	7.228075	7.228205	7.228205	7.228205
13	400	6.827500	6.995044	6.994489	6.994488	6.994488
14	500	7.400100	7.229221	7.228652	7.228652	7.228652
15	600	6.213300	6.129374	6.129400	6.129400	6.129400
16	700	5.918600	5.883923	5.884121	5.884121	5.884121
17	800	4.542600	4.542873	4.543127	4.543127	4.543127
18	900	4.126300	4.153784	4.154020	4.154020	4.154020
19	1000	3.311200	3.362894	3.363075	3.363075	3.363075

Table 4. Change of ($S_k + \Delta S_k^{(j)}$) (ppt) at each iteration using the Newton's method. It is noted that the iteration converges at the third iteration.

k	Depth (m)	j = 0	j = 1	j = 2	j = 3	j =4
1	0	34.424300	34.421995	34.421985	34.421985	34.421985
2	10	34.427800	34.420749	34.420765	34.420765	34.420765
3	20	34.288000	34.299459	34.299526	34.299526	34.299526
4	30	34.291400	34.298031	34.298045	34.298045	34.298045
5	50	34.299100	34.303105	34.303102	34.303102	34.303102
6	75	34.307300	34.309152	34.309141	34.309141	34.309141
7	100	34.328000	34.327896	34.327883	34.327883	34.327883
8	125	34.360400	34.358223	34.358213	34.358213	34.358213
9	150	34.369600	34.364978	34.364978	34.364978	34.364978
10	200	34.336400	34.335234	34.335222	34.335222	34.335222
11	250	34.341500	34.340005	34.339993	34.339993	34.339993
12	300	34.336700	34.333394	34.333388	34.333388	34.333388
13	400	34.285200	34.276792	34.276820	34.276820	34.276820
14	500	34.312300	34.320875	34.320904	34.320904	34.320904
15	600	34.402200	34.406412	34.406410	34.406410	34.406410
16	700	34.486800	34.488540	34.488530	34.488530	34.488530
17	800	34.490400	34.490386	34.490374	34.490374	34.490374
18	900	34.455800	34.454421	34.454409	34.454409	34.454409
19	1000	34.475500	34.472906	34.472897	34.472897	34.472897

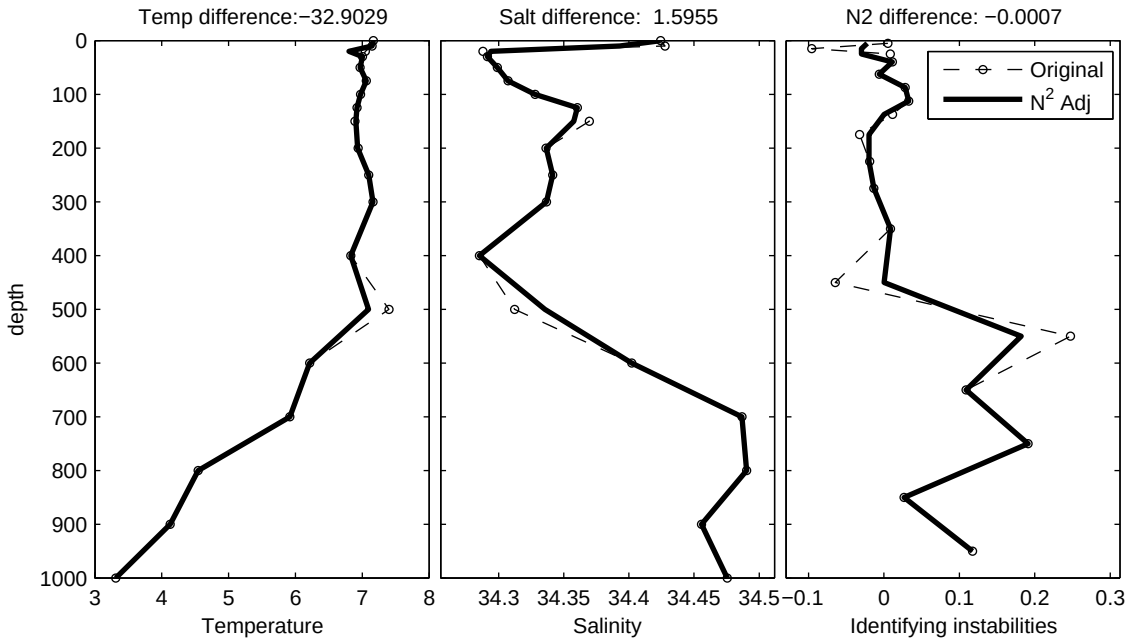

Fig. 1. Original (dashed) and adjusted (solid) profiles temperature (T_k), salinity (S_k), and static stability (E_k) at the grid box 171.5°E, 53.5°E using the JM method (Locarnini et al. 2006).

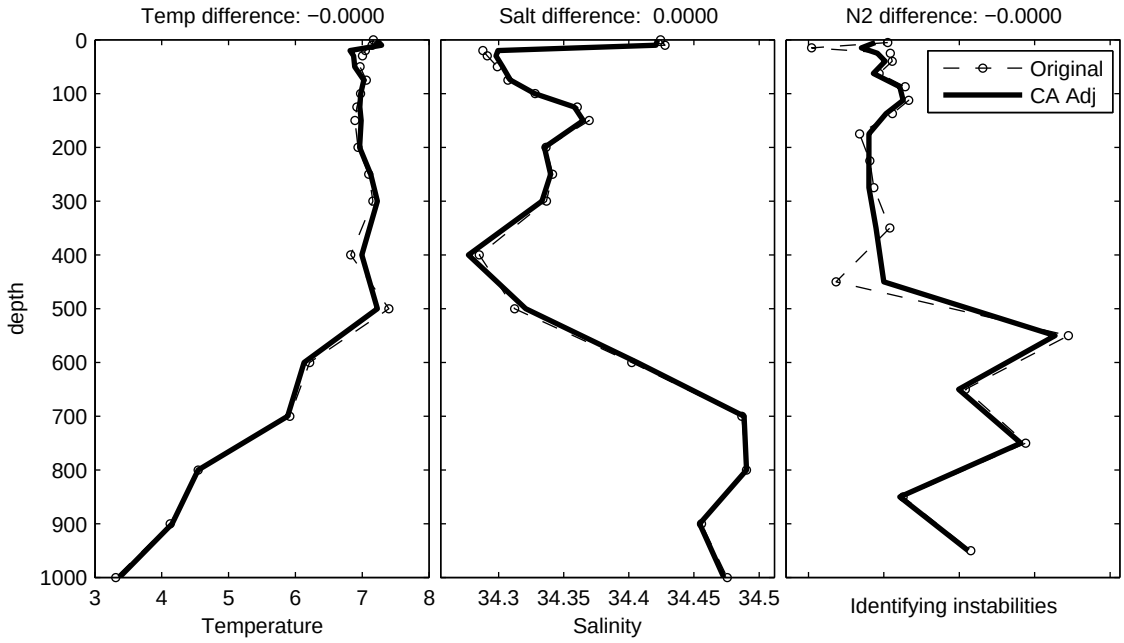

Fig. 2. Original (dashed) and adjusted (solid) profiles temperature (T_k), salinity (S_k), and static stability (E_k) at the grid box 171.5°E, 53.5°E using the analytical conserved method proposed in this paper.

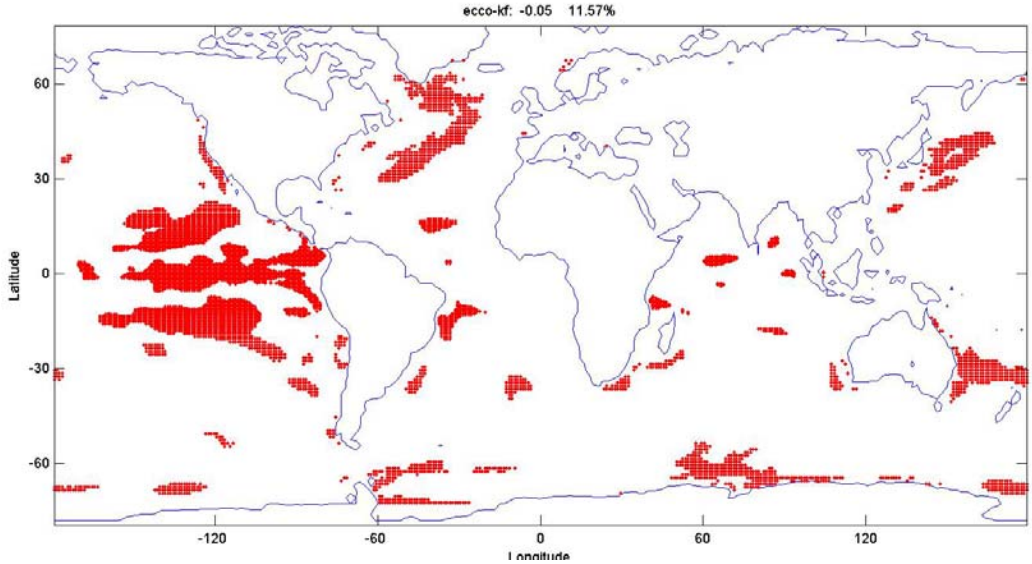

Fig. 3. Distribution of statically unstable casts in the JPL-ECCO 10-day data centered on December 31, 2008. The data were produced by a data assimilation system.

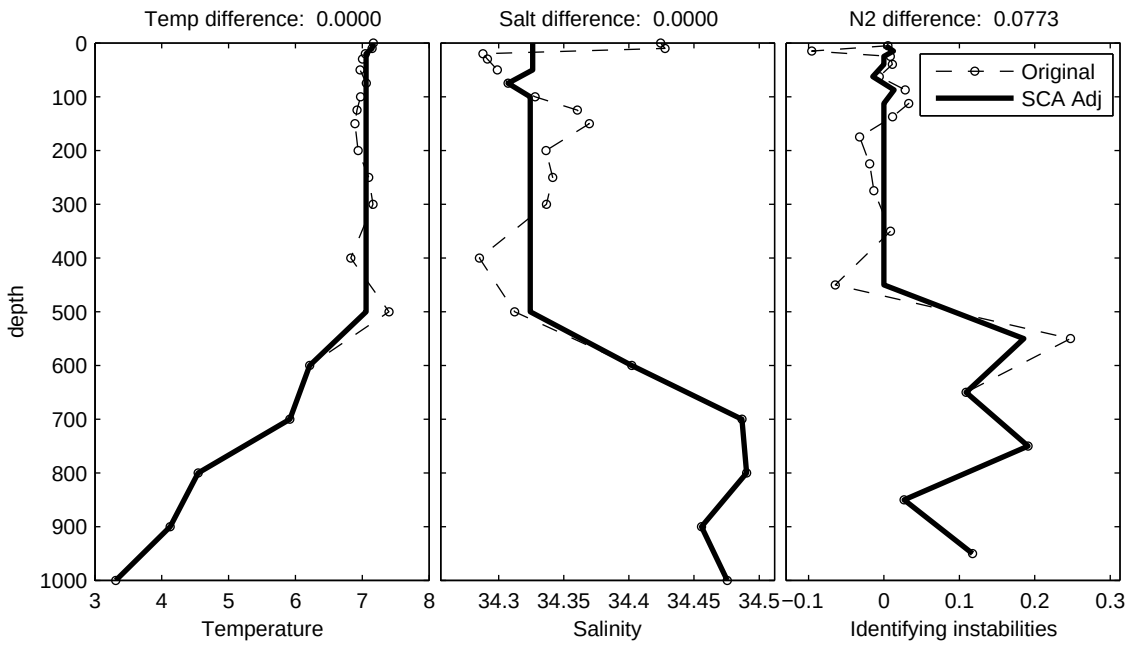

Fig. 4. Original (dashed) and adjusted (solid) profiles temperature (T_k), salinity (S_k), and static stability (E_k) at the grid box 171.5°E, 53.5°E using the complete convective adjustment method (Yin and Sarachik Locarnini 1994).